Available online at www.sciencedirect.com
ScienceDirect
Icarus 190 (2007) 573–584
ICARUS
www.elsevier.com/locate/icarus

Shapes of the saturnian icy satellites and their significance

P.C. Thomas [a,*], J.A. Burns [a], P. Helfenstein [a], S. Squyres [a], J. Veverka [a], C. Porco [b], E.P. Turtle [c], A. McEwen [d], T. Denk [e], B. Giese [f], T. Roatsch [f], T.V. Johnson [g], R.A. Jacobson [g]

[a] *Center for Radiophysics and Space Research, Cornell University, Ithaca, NY 14853, USA*
[b] *Space Science Institute, 4750 Walnut Street, Boulder, CO 80301, USA*
[c] *Johns Hopkins University Applied Physics Laboratory, 11100 Johns Hopkins Rd., Laurel, MD 20723, USA*
[d] *Department of Planetary Sciences, University of Arizona, Tucson, AZ 85721, USA*
[e] *Institut für Geologische Wissenschaften, Freie Universität, 12249 Berlin, Germany*
[f] *Institute of Planetary Research, German Aerospace Center, Rutherfordstrasse 2, 12489 Berlin, Germany*
[g] *Jet Propulsion Laboratory, California Institute of Technology, 4800 Oak Grove Drive, Pasadena, CA 91109, USA*

Received 21 August 2006; revised 9 March 2007

Available online 4 April 2007

Abstract

The sizes and shapes of six icy saturnian satellites have been measured from Cassini Imaging Science Subsystem (ISS) data, employing limb coordinates and stereogrammetric control points. Mimas, Enceladus, Tethys, Dione and Rhea are well described by triaxial ellipsoids; Iapetus is best represented by an oblate spheroid. All satellites appear to have approached relaxed, equilibrium shapes at some point in their evolution, but all support at least 300 m of global-wavelength topography. The shape of Enceladus is most consistent with a homogeneous interior. If Enceladus is differentiated, its shape and apparent relaxation require either lateral inhomogeneities in an icy mantle and/or an irregularly shaped core. Iapetus supports a fossil bulge of over 30 km, and provides a benchmark for impact modification of shapes after global relaxation. Satellites such as Mimas that have smoother limbs than Iapetus, and are expected to have higher impact rates, must have relaxed after the shape of Iapetus was frozen.

Keywords: Saturn, satellites; Satellites, shapes; Interiors

1. Introduction

Saturn's system of satellites includes seven approximately ellipsoidal objects and dozens of smaller ones with irregular shapes. The larger satellites display a wide range of surface features, albedos, and mean densities. Ellipsoidal objects may be equilibrium shapes determined by their mean density, mass distribution, and spin rates (Chandrasekhar, 1969; Dermott, 1979), and as such their shapes may contain information on their interiors. Likewise, departures from equilibrium forms may reveal information on processes that complicate or defeat tendencies to relax to equilibrium shapes. Cassini data permit measurement of the shapes and masses of most of the ellipsoidal satellites sufficiently well to test models of the interior structure and the extent of relaxation.

In this work we first review the method of shape determination and evaluation. Next we report the measurement results for six satellites (Fig. 1). We then examine how close each moon is to an equilibrium shape. Then we view the results in toto, and finally evaluate the significance of departures from equilibrium forms. We do not consider the largest satellite Titan, as ISS cannot detect the satellite's surface limb and shape measurement requires a global network of control points, which are not yet available.

2. Methods and data

2.1. Shape measurement

The overall shapes are found by measuring limb positions in the ISS images. The process involves these steps: (1) Mea-

* Corresponding author.
E-mail address: pct2@cornell.edu (P.C. Thomas).

0019-1035/$ – see front matter
doi:10.1016/j.icarus.2007.03.012

sure the coordinates of limbs to ∼0.1 pixels in the images by techniques described in Thomas et al. (1998). (2) Remove camera distortions and scale limb positions to distance (now given in km) from an approximate center in the image plane. (3) Test if individual limbs are well fit by ellipses. (4) Combine views from different orientations and test for the best-fit ellipsoid and adjust centers in all the images. (5) Examine residuals from the fit ellipsoid to see if an ellipsoid approximation is appropriate. (6) Compare the ellipsoid to equilibrium forms.

The resolution of the images, in pixels/diameter, is sufficiently good that most of a shape's uncertainty derives from the topography, i.e., the deviations from perfect ellipsoidal outlines. Topography on the ellipse can bias centering and thus affect the overall solution. The best images would be 360° limb arc views which highly constrain the center. Views that include transits across Saturn, or include Saturnshine on the dark limb, provide data with more than 180° of arc and greatly reduce the centering uncertainties. In the absence of transits or Saturnshine, low phase angles that provide at least 180° of arc are required. Our techniques also require having the entire limb within one ISS frame (1024 × 1024 pixels). The ellipsoid axes (a, b, c) are found by comparing each image's limb coordinates to the predicted projected ellipse given the ellipsoid shape and camera orientation and viewpoint relative to the object's axes (see (Dermott and Thomas, 1988) for ellipsoidal projections and fitting ellipses). Residuals are the radial differences in pixels between predicted and observed limb positions.

2.2. Evaluation of uncertainties

We use a formal method of uncertainty calculation, checked by other estimates. The accuracy of the limb-finding software can be evaluated by comparing results from images of very different resolution. Enceladus images having better than 2 km/pixel scale and those with 16 km/pixel scale give mean radii differing by 1.3 km. In combination with results from very low-resolution data taken of the Galilean satellites (known sizes), we conclude that uncertainties due to the limb-finding algorithm are ∼0.1 pixels. The precision is frequently of order 0.05 pixels. For most fits this uncertainty is small compared to the uncertainty introduced by roughness of the topography. To determine the allowable range of solutions for a, b, c axes, the residuals calculated in pixels were allowed to increase above the minimum by an unrelated 0.1 pixels, equivalent to the measurement uncertainty. The resulting range of allowed solutions depends upon the image resolutions, limb roughnesses, and spacing of the observed limbs around the object. Uncertainties in $(a - c)$ do not equal sums of the uncertainties in a and c because the solutions of the different axes are, to varying degrees, linked in the various data sets. That is, the maximum $(a - c)$ is not necessarily the difference of the maximum a and the minimum c allowed.

We have also used partial data sets to evaluate the uncertainties of not employing all of the limb; these errors can cause fit centers to vary, hence affect the fit axes. For Mimas, removing about 10% of the data points from the ends of profiles changed all three fit axes by 0.1 km. For Enceladus the data were also split into those with pixel scales greater than 2 km and those less than 2 km. Solutions with each set were within 0.2 km for all axes, and mean radii varied by only 0.1 km. We conclude that the formal errors listed in Table 1 are reasonable limits on the values measured. The uncertainties reported in Table 1 are those developed from our formal testing of residuals, and should be regarded as 2-sigma uncertainties. They do not account for uncertainties in the envelope correction; however, as noted in the following paragraph, the practical effect of such uncertainties is not significant to our main conclusions.

Because limbs are envelopes over the high topography, we have applied corrections to account for hidden depressions (crater interiors) so that the axes and mean radii are appropri-

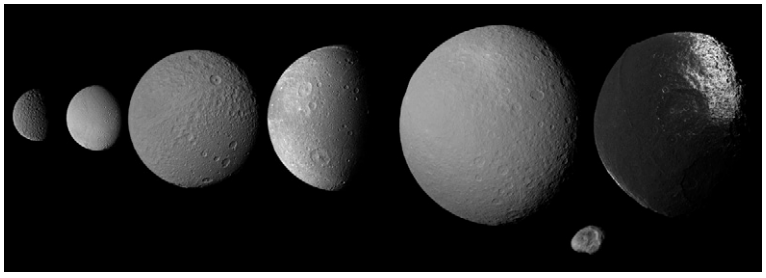

Fig. 1. Ellipsoidal icy satellites with Hyperion as an example of an irregularly shaped satellite. From left: Mimas, Enceladus, Tethys, Dione, Rhea, Hyperion, Iapetus.

Table 1
Satellite shapes

Satellite	a	b	c	Mean radius	$a - c$ (km)	Im	Data
Mimas	207.4 ± 0.7	196.8 ± 0.6	190.6 ± 0.3	198.2 ± 0.5	16.8 ± 0.6	18	11,187
Enceladus	256.6 ± 0.6	251.4 ± 0.2	248.3 ± 0.2	252.1 ± 0.2	8.3 ± 0.6	26	19,027
Tethys	540.4 ± 0.8	531.1 ± 2.6	527.5 ± 2.0	533.0 ± 1.4	12.9 ± 1.9	7	3003
Dione	563.8 ± 0.9	561.0 ± 1.3	560.3 ± 1.3	561.7 ± 0.9	3.5 ± 1.2	14	8184
Rhea	767.2 ± 2.2	762.5 ± 0.8	763.1 ± 1.1	764.3 ± 2.2	4.1 ± 2.1	22	17,402
Iapetus	747.4 ± 3.1		712.4 ± 2.0	735.6 ± 3.0	35.0 ± 3.7	39	10,316

Note. Here we use a, b, c (all in km) to denote the Saturn-facing, orbit-facing, and polar radii. Im: number of images used; Data: number of data points.